24. McArdel, C. A., Franklin, J., Green, L. & Hislop, J. N. Signaling, cycling and desensitization of gonadotrophin-releasing hormone receptors. *J. Endocrinol.* **173,** 1–11 (2002).
25. Rhee, S. G. Regulation of phosphoinositides-specific phospholipase C. *Annu. Rev. Biochem.* **70,** 281–312 (2001).
26. McPherson, P. S. *et al.* A presynaptic inositol-5-phosphatase. *Nature* **379,** 353–357 (1996).
27. Wenk, M. R. *et al.* PIP kinase Iγ is the major PI(4,5)P_2 synthesizing enzyme at the synapse. *Neuron* **32,** 79–88 (2001).
28. Cremona, O. & De Camilli, P. Phosphoinositides in membrane traffic at the synapse. *J. Cell Sci.* **114,** 1041–1052 (2001).
29. Lu, T., Nguyen, B., Zhang, X.-M. & Yang, J. Architecture of a K^+ channel inner pore revealed by stoichiometric covalent modification. *Neuron* **22,** 571–580 (1999).
30. Yang, J. & Tsien, R. W. Enhancement of N- and L-type calcium channel currents by protein kinase C in frog sympathetic neurons. *Neuron* **10,** 127–136 (1993).

Supplementary Information accompanies the paper on *Nature*'s website (http://www.nature.com/nature).

Acknowledgements We thank S. Siegelbaum for comments on the manuscript; Y. Mori for $Ca_v2.1$ cDNA; E. Perez-Reyes for β4 cDNA; T. Tanabe for α2δ cDNA; D. J. Julius for p75 and TrkA (wild-type and mutant) cDNAs. This work was supported by a grant to J.Y. from the National Heart, Lung, and Blood Institute. J.Y. is a recipient of the McKnight Scholar Award and the Scholar Research Programme of the EJLB Foundation.

Competing interests statement The authors declare that they have no competing financial interests.

Correspondence and requests for materials should be addressed to J.Y. (e-mail: jy160@columbia.edu).

Thiamine derivatives bind messenger RNAs directly to regulate bacterial gene expression

Wade Winkler*, Ali Nahvi† & Ronald R. Breaker*

** Department of Molecular, Cellular and Developmental Biology, and*
† Department of Molecular Biophysics and Biochemistry, Yale University, PO Box 208103, New Haven, Connecticut 06520-8103, USA

Although proteins fulfil most of the requirements that biology has for structural and functional components such as enzymes and receptors, RNA can also serve in these capacities. For example, RNA has sufficient structural plasticity to form ribozyme[1,2] and receptor[3,4] elements that exhibit considerable enzymatic power and binding specificity. Moreover, these activities can be combined to create allosteric ribozymes[5,6] that are modulated by effector molecules. It has also been proposed[7–12] that certain messenger RNAs might use allosteric mechanisms to mediate regulatory responses depending on specific metabolites. We report here that mRNAs encoding enzymes involved in thiamine (vitamin B_1) biosynthesis in *Escherichia coli* can bind thiamine or its pyrophosphate derivative without the need for protein cofactors. The mRNA–effector complex adopts a distinct structure that sequesters the ribosome-binding site and leads to a reduction in gene expression. This metabolite-sensing regulatory system provides an example of a 'riboswitch' whose evolutionary origin might pre-date the emergence of proteins.

A thiamine pyrophosphate (TPP)-dependent sensor/regulatory protein has been proposed to participate in the control of thiamine biosynthetic genes[13], but thus far no such protein factor has been shown to exist. Recently, we established that the mRNA leader sequence of the *btuB* gene of *E. coli* can bind coenzyme B_{12} selectively, and that this binding event brings about a structural change in the RNA that is important for genetic control[14]. In the current study, we set out to determine whether mRNAs that encode thiamine biosynthetic proteins might also use a riboswitch that is located in their untranslated leader sequence. We prepared β-galactosidase translational fusion constructs that encompass the 5′-untranslated regions of *thiM* and *thiC* mRNAs of *E. coli*, each of which includes a previously identified '*thi* box' domain whose sequence and potential secondary structure are conserved in several species of bacteria and archaea[11]. The *thiM* and *thiC* translational fusion constructs exhibit thiamine-dependent suppression of β-galactosidase activity of 18- and 110-fold, respectively, when host cells are grown in a minimal medium. A transcriptional fusion containing the *thiM* leader is not subject to suppression by thiamine, but a similar fusion with *thiC* leader yields a 16-fold modulation with thiamine, suggesting that a significant portion of genetic control observed with *thiC* occurs at the level of transcription.

These constructs were subsequently used to prepare DNA templates by polymerase chain reaction (PCR) for *in vitro* transcription of RNA fragments. The resulting RNAs were subjected to a structure-probing process[14–16] to reveal whether the RNAs undergo structure modulation upon binding of ligands. Internucleotide linkages in unstructured regions are more likely to undergo spontaneous cleavage compared to linkages that reside in highly structured regions of an RNA[15]. The 165-nucleotide *thiM* RNA fragment (165 *thiM*) has a distinct pattern of cleavage products that is generated when the RNA is incubated for an extended period in the absence of TPP (Fig. 1a). Upon addition of 100 μM TPP, 165 *thiM* undergoes substantial structural alteration, with many internucleotide linkages in the region spanning positions 39–80 exhibiting a reduction in spontaneous cleavage. This indicates that TPP binds to the RNA and stabilizes a defined structure within this region, resulting in a lower rate of fragmentation.

The fragmentation patterns are largely congruent with potential stem and bulge structures that are identified by a secondary-structure prediction algorithm[17,18]. Most linkages that experience a ligand-induced reduction of cleavage are encompassed by the *thi* box and nucleotides that reside immediately 5′ relative to this domain (Fig. 1b). Other linkages that undergo cleavage, but that are not modulated by TPP, are predicted to reside in bulges or in the loops of hairpins. Predicted base-paired structures labelled P2–P7 include linkages that exhibit the lowest levels of spontaneous cleavage, implying that they remain structured in both the presence and absence of TPP. Nucleotides 126–130 encompass the only region apart from those described above that becomes more structured upon TPP addition. These nucleotides correspond to the Shine–Dalgarno (SD) sequence, which is required to be unpaired for efficient translation of mRNAs in prokaryotes. These findings are consistent with a genetic control mechanism in which the *thiM* RNA binds to TPP and forms a complex such that the ribosome cannot gain access to the SD sequence.

Similarly, structure probing was used to examine the mRNA leader for *thiC*. The 240 *thiC* RNA also exhibits extensive modulation of its pattern of spontaneous cleavage, and again the majority of the changing pattern is located in the *thi* box and in the region located immediately upstream of this domain (Fig. 1c). These regions of highest structure modulation in *thiM* and *thiC* can be folded into similar secondary structures (Fig. 1d), and carry several common sequence elements within and adjacent to the *thi* box domain. Therefore, we propose that the structures of *thiM* and *thiC* spanning stems P1–P5 comprise TPP-binding motifs that are analogous to aptamers, which are engineered ligand-binding RNAs[3,4,19]. Nucleotides residing 3′ relative to this natural TPP aptamer are probably involved in converting the metabolite binding event into a genetic response (see below).

The sensitivity of metabolite detection by these mRNAs was assessed by establishing apparent dissociation constant (apparent K_D) values for TPP, thiamine, and thiamine monophosphate (TP). Values were generated by monitoring the extent of spontaneous cleavage at several ligand-sensitive sites within the RNA over a range

of ligand concentrations. For example, probing of a trace amount of 165 *thiM* RNA with TPP concentrations ranging from zero to 100 μM (or up to 10 mM with certain analogues) reveals that half-maximal modulation of RNA structure occurs when approximately 600 nM TPP is present (Fig. 2a), which reflects an apparent K_D of 600 nM. Likewise, probing of 240 *thiC* reveals an apparent K_D of 100 nM. Both 165 *thiM* and 240 *thiC* RNAs appear to bind TPP more readily than TP or thiamine, with *thiC* exhibiting more than 1,000-fold discrimination against TP and thiamine (Fig. 2b). The fact that TPP is the strongest modulator of RNA structure is consistent with genetic observations in *Salmonella typhimurium* that TPP synthesis is required for regulation of expression of thiamine biosynthesis genes[20]. The differential specificity achieved by the RNAs, which is a phenomenon that is commonly observed for receptor–ligand systems made of protein, indicates that these ligand-binding RNAs might be amenable to specificity changes through evolutionary forces.

It is important to note that the actual K_D values for RNA–ligand interactions might be different inside cells where physiological conditions of Mg^{2+} and other agents that can influence RNA structure will not match those of our assays. Also, the nature of the RNA construct can be a source of an altered K_D. For example, we found that the minimized 91 *thiM* construct (Fig. 1a), which largely encompasses only the putative natural aptamer, retains the ability to bind TPP and exhibits an apparent K_D that is improved by ~20 fold compared to the longer construct (Fig. 2b). Thus, the affinity for TPP might vary as the nascent RNA transcript emerges from the active site of RNA polymerase or the ribosome. Furthermore, this result demonstrates that the 91 *thiM* aptamer can be separated from RNA components (collectively termed the 'expression platform') that are directly controlling gene expression. This modular construction, involving the physical and functional separation of aptamer and expression platform domains, would be expected to facilitate the generation of TPP-controlled RNAs through evolutionary processes or by rational RNA engineering strategies.

We noticed that spontaneous cleavage at several linkages within the *thi* box domain of 165 *thiM* specifically correlate with the type of ligand used. Although TPP reduces spontaneous cleavage of 165 *thiM* at nucleotides A61, U62 and, to a smaller extent, at U79, these same sites retain an elevated level of cleavage when thiamine is present near its saturating concentration (Fig. 2c). These nucleotides cluster at an internal bulge within the *thi* box domain, and could be contributing to the binding site for the phosphate groups of TPP.

To further explore the molecular recognition characteristics of the TPP riboswitch, we examined the structural modulation of 165 *thiM* in the presence of several analogues that carry certain structural features of thiamine (Fig. 3a). Thiamine, TP and TPP induce modulation as expected (Fig. 3b). However, oxythiamine and other thiamine analogues with less similarity to TPP fail to induce structure modulation. The performance of this sampling of analogues indicates that the RNA makes specific contacts to distal parts of its ligand, and that both the purine and phosphate groups carry important elements for molecular recognition (Fig. 3c). Similar results are obtained by using equilibrium dialysis assays (Fig. 3d). For example, the addition of 91 *thiM* RNA to chamber *b* of an

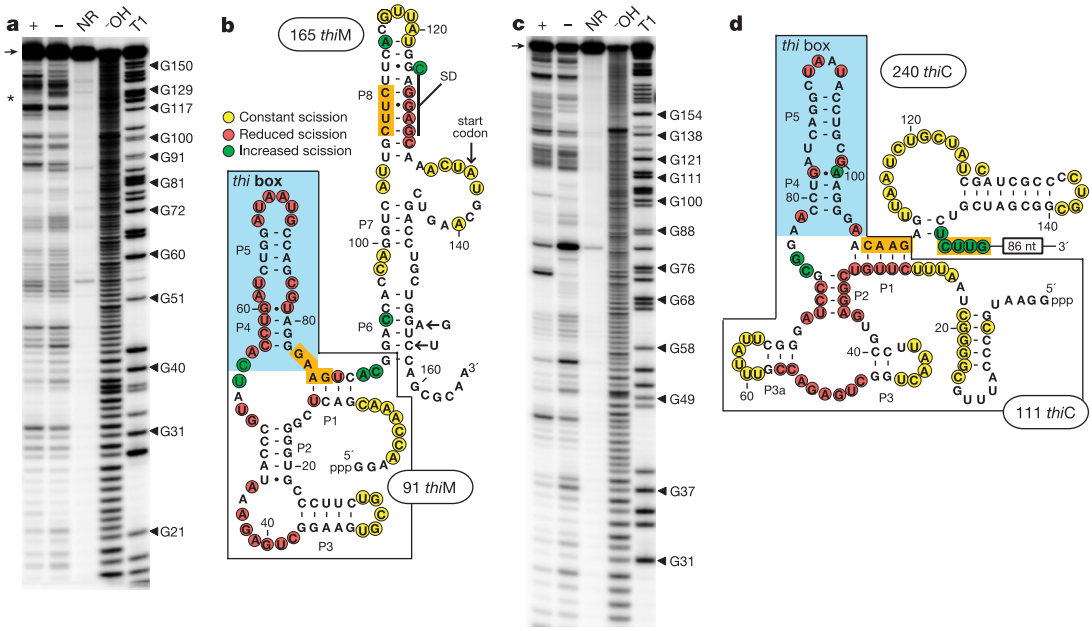

Figure 1 Metabolite binding by mRNAs. **a**, Thiamine pyrophosphate (TPP)-dependent modulation of the spontaneous cleavage of 165 *thiM* RNA visualized by polyacrylamide gel electrophoresis (PAGE). 5′ ^{32}P-labelled RNAs (arrow, 20 nM) were incubated for ~40 h at 25 °C in 20 mM $MgCl_2$, 100 mM KCl, and 50 mM Tris–HCl (pH 8.3 at 25 °C) in the presence (+) or absence (–) of 100 μM TPP. NR, $^{-}$OH and T1 represent RNAs subjected to no reaction, partial digestion with alkali, or partial digestion with RNase T1 (G-specific cleavage), respectively. Product bands corresponding to cleavage after selected G residues are numbered and identified by filled arrowheads. The asterisk identifies modulation of RNA structure involving the Shine–Dalgarno (SD) sequence. Gel separations were analysed using a phosphorimager (Molecular Dynamics) and quantified using ImageQuant software. **b**, Secondary-structure model of 165 *thiM* as predicted by computer modelling[17,18] and by the structure-probing data depicted in **a**. Unmarked nucleotides exhibit a constant but low level of degradation. The truncated 91 *thiM* RNA is boxed, and the *thi* box element[11] is shaded light blue. Nucleotides highlighted in orange identify a possible alternative pairing, designated P8*. The RNA carries two mutations (G155A and U157C) relative to wild type that were introduced in a non-essential portion of the construct to form a restriction site for cloning, while all RNAs carry two 5′-terminal G residues to facilitate *in vitro* transcription. **c**, TPP-dependent modulation of the spontaneous cleavage of 240 *thiC* RNA. Reactions were conducted and analysed as described in **a**. **d**, Secondary-structure model of 240 *thiC*. Potential base-paired elements that are similar to those of *thiM* are labelled P1–P5. The truncated RNA 111 *thiC* is boxed. Nucleotides highlighted in orange identify a possible alternative pairing. Additional details are as described in **b**.

equilibrium dialysis assembly (see Methods) causes a shift in the distribution of ^{3}H-thiamine in favour of chamber *b*, unless an excess of unlabelled TPP is also included. However, the presence of oxythiamine does not significantly restore the tritium distribution to unity, which is expected because probing data indicate that it is not able to bind the RNA. These findings imply that the aptamer domain of the TPP riboswitch is highly selective for its target ligand.

The secondary-structure model for 165 *thiM* RNA was examined in greater detail by generating and testing a series of variant constructs (Fig. 4a). For example, variant M1 carries a mutation that disrupts the predicted P3 pairing element. This mutation causes a loss of TPP binding (Fig. 4b; for example, see position C77) and a loss of genetic control of the corresponding β-galactosidase fusion construct (Fig. 4b, bottom). Restoration of base pairing in the double-mutant construct M2 restores both TPP binding and genetic control. Similarly, disruptive and restorative mutations encompassed by constructs M3–M6 are consistent with the formation of stems P5 and P8 (Fig. 4c). Upon the addition of TPP, the SD element of both the wild-type and M2 constructs becomes sequestered in a structure that precludes a high level of spontaneous cleavage. In contrast, the M1 construct does not exhibit SD modulation (Fig. 4b, nucleotides 126–130). These results suggest that the genetic switch might be turned off by a mechanism whereby TPP binding ultimately promotes the stable formation of P8, which reduces access to the SD by the ribosome.

We observed that the predicted partner of the SD sequence in P8 (nucleotides 108–111) remains resistant to spontaneous cleavage both in the presence and absence of TPP (Fig. 1a). This suggests that, upon addition of TPP, the formation of P8 might be due to the displacement of an alternative structure that otherwise prevents this anti-SD element from forming P8. Furthermore, we noticed that nucleotides 83–86 are complementary to the anti-SD element, and that this region also resists spontaneous cleavage in the presence and absence of TPP. One mechanism by which genetic control could result is by way of the mutually exclusive formation of P8* (Fig. 1b) in the 'on' state versus the simultaneous formation of P1 and P8 in

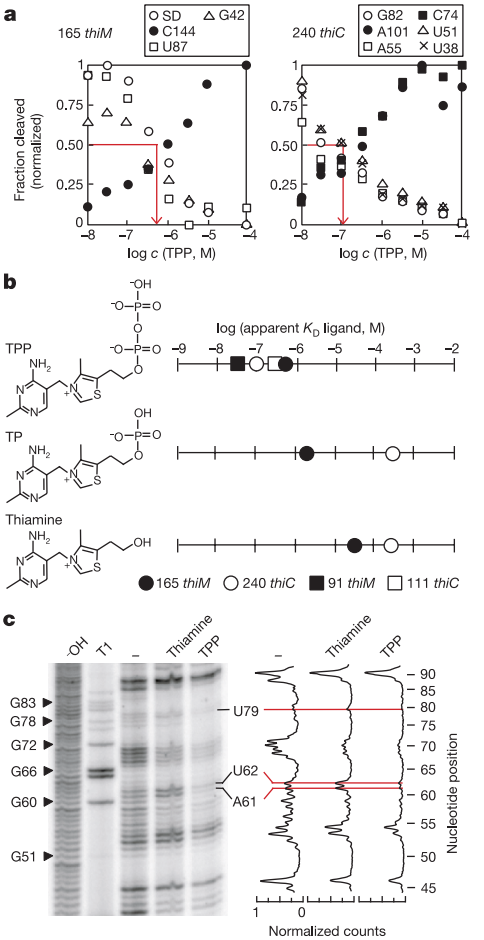

Figure 2 The *thiM* and *thiC* mRNA leaders serve as high-affinity metabolite receptors. **a**, The extent of spontaneous RNA cleavage at several sites within 165 *thiM* (left) and 240 *thiC* (right) are plotted for different concentrations (*c*) of TPP. Red arrows reflect the estimated concentration of TPP needed to attain half maximal modulation of RNA (apparent K_D). **b**, The logarithm of the apparent K_D values are plotted for both RNAs with TPP, TP (thiamine monophosphate) and thiamine as indicated. **c**, Patterns of spontaneous cleavage of 165 *thiM* differ between thiamine and TPP ligands as depicted by PAGE analysis (left) and as reflected by graphs (right) representing the relative phosphorimager counts for the three lanes as indicated. Peaks corresponding to the identified bands are highlighted by coloured lines. Details for the RNA probing analysis are similar to those described in Fig. 1a. The graphs were generated by ImageQuant software.

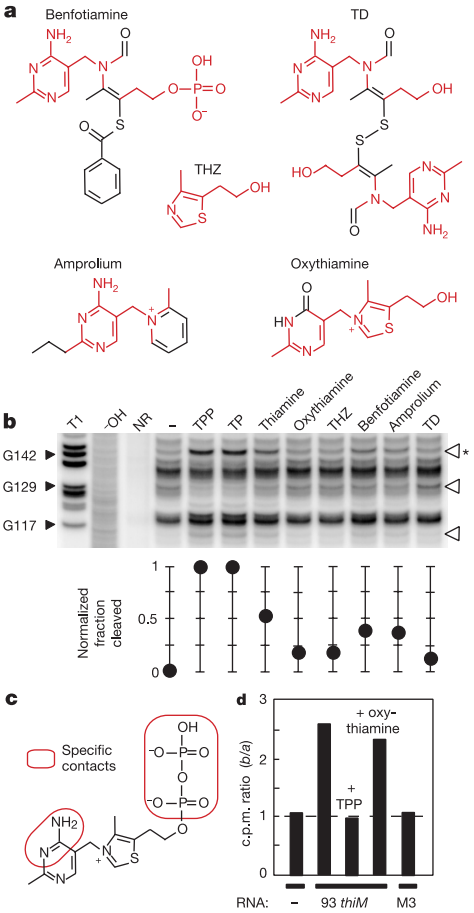

Figure 3 High sensitivity and selectivity of mRNA leaders for metabolite binding. **a**, Chemical structures of several analogues of thiamine. (TD, thiamine disulphide; THZ, 4-methyl-5-β-hydroxyethylthiazole.) Structures in red are similar to TPP. **b**, PAGE analysis of 165 *thiM* RNA structure probing using TPP and various chemical analogues (40 μM each) as indicated. Locations of significant structural modulation within the RNA spanning nucleotides ~113 to ~150 are indicated by open arrowheads. The asterisk identifies the site (C144) used to compare the normalized fraction of RNA that is cleaved (bottom) in the presence of specific compounds. Details for the RNA probing analysis are similar to those described in Fig. 1a. **c**, Summary of the features of TPP that are critical for molecular recognition. **d**, Equilibrium dialysis using ^{3}H-thiamine as a tracer. Plotted are the ratios for tritium distribution in a two-chamber system (*a* and *b*) that were established upon equilibration in the presence of the RNA constructs in chamber *b* as indicated (see Fig. 4 for a description of the non-TPP-binding mutant M3). 100 μM TPP or oxythiamine was added to chamber *a*, as denoted, upon the start of equilibration.

the metabolite-bound 'off' state (Fig. 5). A genetic control strategy of alternative structure formation would be similar to that found in mRNAs that use terminator, antiterminator, and anti-antiterminator structural elements.

In a preliminary assessment of this mechanism, we tested constructs M7–M9. Construct M7 carries a U109C mutation in the anti-SD sequence that is expected to destabilize the P8 interaction while simultaneously destabilizing the P8* interaction. M7 retains TPP binding function and exhibits a significant level of genetic modulation (Fig. 4c), which is expected if the mutation does not disrupt the relative distribution of mRNAs between the 'on' and 'off' states. In comparison, M8 (U110C) retains TPP binding, exhibits a marked reduction in the level of reporter expression, and loses nearly all genetic modulation. In addition, M8 no longer exhibits detectable spontaneous cleavage in the SD sequence, which is consistent with the prediction that the thermodynamic balance between P8 and P8* formation should be shifted decidedly in favour of P8 in this RNA variant. Construct M9, which carries four mutations in the anti-SD element, has a significantly different pattern of spontaneous cleavage in the SD region. Not surprisingly, M9 fails to reduce gene expression upon thiamine addition to cells, despite the fact that the construct retains TPP binding activity *in vitro*. Although a more detailed analysis is needed to confirm this model, it is evident from these data that TPP binding restricts the structural freedom of the SD element in the appropriate RNA variants, and that this correlates with genetic control.

The biochemical and genetic data reported here show that certain mRNAs carry natural aptamer domains, and that binding of specific metabolites directly to these RNA domains leads to modulation of gene expression. RNA structure-probing data indicate that the TPP riboswitch operates as an allosteric sensor of its target compound—binding of TPP by the aptamer domain stabilizes a conformational state within the aptamer and within the neighbouring expression platform that precludes translation. The diversity of expression platforms seems to be large. Our findings suggest that the *thiM* RNA uses a SD-blocking mechanism to control translation. In contrast, the *thiC* RNA controls gene expression both at transcription and translation, and therefore might make use of a more complex expression platform that converts TPP binding into a transcription termination event and into inhibition of translation of completed mRNAs.

In addition to the TPP-sensing system that we describe here, and a newly discovered riboswitch[14] that functions with coenzyme B_{12}, we also have evidence that the *RFN* element[21] (a conserved RNA sequence found in certain bacterial mRNAs) serves as a flavin mononucleotide-dependent riboswitch (unpublished data).

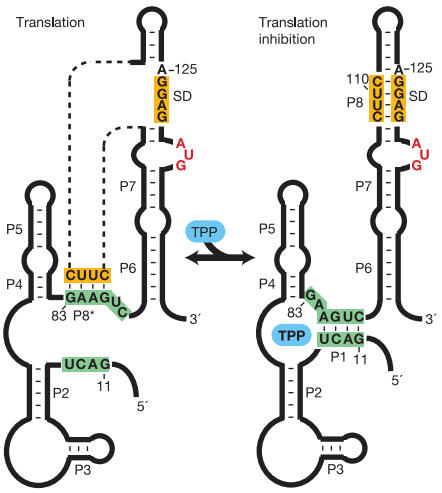

Figure 5 Schematic representation of the proposed mechanism for TPP-dependent deactivation of *thiM* translation. In the absence of TPP, the P8* pairing is formed between the anti-SD element and the anti-anti-SD element. This conformation permits the SD sequence to interact with the ribosome, and thus translation proceeds. In the presence of TPP (blue), the obligate formation of the P1 stem sequesters a portion of the anti-anti-SD element, and therefore the complete P8 stem also forms. This precludes ribosome access to the SD element, which inhibits translation. Complementary sequence elements that form P1 and P8 are depicted in green and orange, respectively.

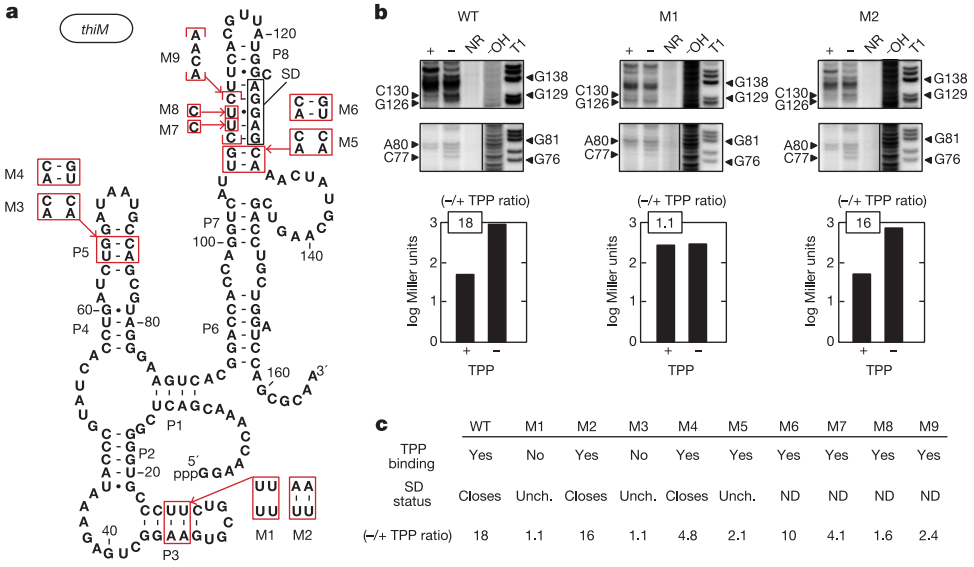

Figure 4 Mutational analysis of the structure and function of the *thiM* riboswitch. **a**, Mutations present in constructs M1–M9 relative to the 165 *thiM* RNA. Boxed nucleotides designate the locations and the identities of the mutations tested. **b**, *In vitro* ligand-binding and genetic control functions of the wild-type (WT), M1 and M2 RNAs as reflected by PAGE analysis of in-line probing experiments (10 μM TPP) and by β-galactosidase expression assays. Labels on gels are as described in Fig. 1a. Bars represent the levels of gene expression in the presence (+) and the absence (−) of TPP in the culture medium. **c**, A summary of analyses (as in **b**) of WT to M9 is presented in table form. The SD status 'closes' signifies that the Shine–Dalgarno sequence exhibits reduced structural flexibility (probably due to P8 formation), while the 'Unch.' designation indicates that the sequence remains structurally unchanged. The SD status 'ND' (not determined) indicates either that the level of spontaneous cleavage detected in the absence and presence of TPP is near the limit of detection (M6, M7 and M8) or that the region adopts an atypical structure (M9) compared to WT.

Although these are (to our knowledge) the first examples of mRNA elements that control genetic expression by metabolite binding, we suspect that they might be only the initial representatives of a genetic control strategy that is widespread in biology. It has been suggested[22–24] that TPP, coenzyme B_{12} and FMN emerged as biological cofactors during the 'RNA world'[25]. If these metabolites were being biosynthesized and used before the advent of proteins, then certain riboswitches might be modern examples of the most ancient form of genetic control. A preliminary search of genomic sequence databases has revealed that sequences corresponding to the TPP aptamer exist in organisms from bacteria, archaea and eukarya—largely without major alteration. Although new metabolite-binding mRNAs are likely to emerge as evolution progresses, it is possible that the known riboswitches are 'molecular fossils' from the RNA world. □

Methods

Chemicals and oligonucleotides

TPP, TP, thiamine, oxythiamine, amprolium and benfotiamine were purchased from Sigma. Thiamine disulphide and THZ were purchased from TCI America. ^{3}H-labelled thiamine was purchased from American Radiolabeled Chemicals, Inc. (10 Ci mmol^{-1}). Synthetic DNAs were synthesized by the Keck Foundation Biotechnology Resource Center at Yale University. DNAs were purified by denaturing (8 M urea) polyacrylamide gel electrophoresis (PAGE), and isolated from the gel by crush-soaking in 10 mM Tris–HCl (pH 7.5 at 23 °C), 200 mM NaCl and 1 mM EDTA. The DNA was recovered by precipitation with ethanol.

Construction of *E. coli thiM–lacZ* and *thiC–lacZ* fusions

The region spanning nucleotides −83 to 238 of the *E. coli thiCEFGH* operon[26] was amplified by PCR from *E. coli* strain MC4100 (a gift from S. Gottesman) as an *Eco*R1-*Bgl*II fragment. The DNA was ligated into *Eco*R1- and *Bam*H1-digested pRS414 plasmid DNA, which contains a promoterless copy of *lacZ* (a gift from R. Simons; ref. 27), resulting in the in-frame fusion of the ninth codon of *lacZ* to the ninth codon of *thiC*. Similarly, the regulatory region of *thiM* (nucleotides −67 to 163) was amplified by PCR as an *Eco*R1-*Bam*H1 fragment and inserted into plasmid pRS414, wherein the sixth codon of *thiM* resides in-frame with the ninth codon of *lacZ*. The plasmids were transformed into Top10 cells (Invitrogen) for all subsequent manipulations. All site-directed mutations were introduced into the *thiC* and *thiM* regulatory regions using the QuikChange site-directed mutagenesis kit (Stratagene) and the appropriate mutagenic DNA primers. All mutations were confirmed by DNA sequencing (USB Thermosequenase).

Thiamine-repression β-galactosidase assays

E. coli cells (Top10, Invitrogen) that contained in-frame *lacZ* fusions to *thiC* or *thiM* mRNA leader sequences, were grown in M9 glucose minimal medium (plus 50 μg ml^{-1} vitamin assay Casamino acids; Difco) to mid-exponential phase. The cultures were grown either with or without added thiamine (100 μM). Aliquots (1 ml) were removed for β-galactosidase enzyme assays, which were conducted in a manner similar to that described by Miller[28]. All experiments were repeated twice and in duplicate, with Miller unit values reflecting the average of these analyses.

In vitro transcription

Templates for *in vitro* transcription of the fragments of *thiC* and *thiM* mRNA leaders were generated by PCR using the appropriate DNA primers and plasmids pRS414thiC or pRS414thiM, respectively. The dinucleotide sequence GG was introduced into the DNA constructs (corresponding to the 5′ terminus of each RNA construct) to facilitate transcription by T7 RNA polymerase. RNAs were prepared by *in vitro* transcription and were 5′ ^{32}P-labelled as described previously[6].

In-line probing of RNA

Determination of apparent K_D values for each construct was achieved by conducting in-line probing of RNA wherein the concentration of the ligand was varied between 10 nM and 100 μM, or up to 10 mM for weakly binding ligands (see Fig. 1a legend for details). Composite plots of the fraction of RNA cleaved at specific sites versus the logarithm of the concentration of ligand (for example, Fig. 2a) were generated to provide an estimate of the apparent K_D. Fraction cleaved values were normalized relative to the highest and lowest cleavage values measured for each site.

Equilibrium dialysis

Equilibrium dialysis experiments were conducted using a DispoEquilibrium Dialyzer (ED-1, Harvard Bioscience), wherein chambers *a* and *b* were separated by a 5,000 dalton molecular mass cut-off membrane. Equilibration was initiated by the addition of 25 μl of equilibration buffer (50 mM Tris–HCl (pH 8.3 at 25 °C), 20 mM $MgCl_2$, 100 mM KCl), containing 100 nM ^{3}H-thiamine, and by the addition of an equal volume of equilibration buffer either without or with 20 μM RNA as indicated to chamber *b*. Equilibrations were allowed to proceed for 10 h at 23 °C, and aliquots were removed from each chamber and quantified by using a liquid scintillation counter.

Received 2 August; accepted 20 September 2002; doi:10.1038/nature01145.
Published online 16 October 2002.

1. Cech, T. R. & Golden, B. L. *The RNA World* (eds Gesteland, R. F., Cech, T. R. & Atkins, J. F.) 321–350 (Cold Spring Harbor Laboratory Press, Cold Spring Harbor, NY, 1998).
2. Breaker, R. R. *In vitro* selection of catalytic polynucleotides. *Chem. Rev.* **97,** 371–390 (1997).
3. Osborne, S. E. & Ellington, A. D. Nucleic acid selection and the challenge of combinatorial chemistry. *Chem. Rev.* **97,** 349–370 (1997).
4. Hermann, T. & Patel, D. J. Adaptive recognition by nucleic acid aptamers. *Science* **287,** 820–825 (2000).
5. Soukup, G. A. & Breaker, R. R. Engineering precision RNA molecular switches. *Proc. Natl Acad. Sci. USA* **96,** 3584–3589 (1999).
6. Seetharaman, S., Zivarts, M., Sudarsan, N. & Breaker, R. R. Immobilized RNA switches for the analysis of complex chemical and biological mixtures. *Nature Biotechnol.* **19,** 336–341 (2001).
7. Gold, L. *et al.* From oligonucleotide shapes to genomic SELEX: novel biological regulatory loops. *Proc. Natl Acad. Sci. USA* **94,** 59–64 (1997).
8. Gold, L., Singer, B., He, Y. & Brody, E. SELEX and the evolution of genomes. *Curr. Opin. Gen. Dev.* **7,** 848–851 (1997).
9. Nou, X. & Kadner, R. J. Adenosylcobalamin inhibits ribosome binding to *btuB* RNA. *Proc. Natl Acad. Sci. USA* **97,** 7190–7195 (2000).
10. Gelfand, M. S., Mironov, A. A., Jomantas, J., Kozlov, Y. I. & Perumov, D. A. A conserved RNA structure element involved in the regulation of bacterial riboflavin synthesis genes. *Trends Genet.* **15,** 439–442 (1999).
11. Miranda-Rios, J., Navarro, M. & Soberón, M. A conserved RNA structure (*thi* box) is involved in regulation of thiamin biosynthetic gene expression in bacteria. *Proc. Natl Acad. Sci. USA* **98,** 9736–9741 (2001).
12. Stormo, G. D. & Ji, Y. Do mRNAs act as direct sensors of small molecules to control their expression? *Proc. Natl Acad. Sci. USA* **98,** 9465–9467 (2001).
13. Webb, E. & Downs, D. Characterization of *thiL*, encoding thiamin-monophosphate kinase, in *Salmonella typhimurium*. *J. Biol. Chem.* **272,** 15702–15707 (1997).
14. Nahvi, A. *et al.* Genetic control by a metabolite-binding mRNA. *Chem. Biol.* **9,** 1043–1049 (2002).
15. Soukup, G. A. & Breaker, R. R. Relationship between internucleotide linkage geometry and the stability of RNA. *RNA* **5,** 1308–1325 (1999).
16. Soukup, G. A., DeRose, E. E., Koizumi, M. & Breaker, R. R. Generating new ligand-binding RNAs by affinity maturation and disintegration of allosteric ribozymes. *RNA* **7,** 524–536 (2001).
17. Zuker, M., Mathews, D. H. & Turner, D. H. *RNA Biochemistry and Biotechnology* (eds Barciszewski, J. & Clark, B. F. C.) 11–43 (NATO ASI Series, Kluwer Academic, Boston, 1999).
18. Mathews, D. H., Sabina, J., Zuker, M. & Turner, D. H. Expanded sequence dependence of thermodynamic parameters improves prediction of RNA secondary structure. *J. Mol. Biol.* **288,** 911–940 (1999).
19. Gold, L., Poliski, B., Uhlenbeck, O. & Yarus, M. Diversity of oligonucleotide functions. *Annu. Rev. Biochem.* **64,** 763–797 (1995).
20. Webb, E., Febres, F. & Downs, D. M. Thiamine pyrophosphate (TPP) negatively regulates transcription of some *thi* genes of *Salmonella typhimurium*. *J. Bacteriol.* **178,** 2533–2538 (1996).
21. Gelfand, M. S., Mironov, A. A., Jomantas, J., Kozlov, Y. I. & Perumov, D. A. A conserved RNA structure element involved in the regulation of bacterial riboflavin synthesis genes. *Trends Genet.* **15,** 439–442 (1999).
22. White, H. B. III Coenzymes as fossils of an earlier metabolic state. *J. Mol. Evol.* **7,** 101–104 (1976).
23. White, H. B. III *The Pyridine Nucleotide Coenzymes* 1–17 (Academic, New York, 1982).
24. Benner, S. A., Ellington, A. D. & Tauer, A. Modern metabolism as a palimpsest of the RNA world. *Proc. Natl Acad. Sci. USA* **86,** 7054–7058 (1989).
25. Joyce, G. F. The antiquity of RNA-based evolution. *Nature* **418,** 214–221 (2002).
26. Vander Horn, P. B., Backstrom, A. D., Stewart, V. & Begley, T. P. Structural genes for thiamine biosynthetic enzymes (*thiCEFGH*) in *Escherichia coli* K-12. *J. Bacteriol.* **175,** 982–992 (1993).
27. Simons, R. W., Houman, F. & Kleckner, N. Improved single and multicopy lac-based cloning vectors for protein and operon fusions. *Gene* **53,** 85–96 (1987).
28. Miller, J. H. *A Short Course in Bacterial Genetics* 72 (Cold Spring Harbor Laboratory Press, Cold Spring Harbor, New York, 1992).

Acknowledgements We thank members of the Breaker laboratory for comments on the manuscript, especially N. Sudarsan for discussions. This work was supported by the NIH and the NSF, and by a fellowship to R.R.B. from the David and Lucile Packard Foundation.

Competing interests statement The authors declare that they have no competing financial interests.

Correspondence and requests for materials should be addressed to R.R.B. (e-mail: ronald.breaker@yale.edu).